

The Influence of Charge Density of Chitosan in the Compaction of the Polyanions DNA and Xanthan

Gjertrud Maurstad,[†] Signe Danielsen,[‡] and Bjørn T. Stokke^{*†}

Biophysics and Medical Technology, Department of Physics, The Norwegian University of Science and Technology, NTNU, NO-7491 Trondheim, Norway, and Department of Oncology, St. Olav's Hospital, University Hospital of Trondheim, Norway

Received October 20, 2006; Revised Manuscript Received January 11, 2007

In this study the relative importance of valence and charge density of the polycation chitosan on the compaction process of DNA and xanthan is investigated. Chitosans with approximately equal valence but differing in their charge density were employed to form polyelectrolyte complexes with the two polyanions. The resulting structures (toroids, rods, and globules) have been visualized by AFM. For DNA–chitosan the complexation process was additionally studied by utilizing the fluorescent probe ethidium bromide. The results show that not only the total charge per chitosan molecule (valence), but also the charge density is important in determining the association with polyanions such as DNA and xanthan. Furthermore, it is demonstrated that the pH at which the complexation takes place is an important parameter in the complexation process, influencing the structures formed.

Introduction

Oppositely charged polyelectrolytes will upon mixing interact electrostatically and form polyelectrolyte complexes (polyplexes),¹ a process that is promoted by an increase in entropy due to release of counterions.^{2,3} This assembly process has recently received increasing interest due to its potential use in gene delivery, as polycation-induced compaction of DNA is one of the possible gene delivery routes under investigation.⁴ The structures resulting from the interaction of the polyions is often described by a “scrambled-egg” model for flexible polyelectrolytes,⁵ while stiffer polyelectrolytes such as DNA is capable of forming well-defined structural complexes such as toroids and rods.^{6–9} Polyplex formation bears resemblance to the solvent-induced polymer collapse, with the local intersegment interaction being induced by oppositely charged polyions. It therefore follows that the valence and structure of the polycation is important in the polycation-induced compaction of, e.g., DNA.¹⁰ The binding constant has been reported to increase with the valence of the ligand binding to an oppositely charged polymer (from $\log K_{\text{obs}} = 0.26$ at valence of 2 to $\log K_{\text{obs}} = 0.77$ at a valence of 10).¹¹ The importance of charge has also been emphasized in a number of transfection studies, with increased transfection efficiency following a reduction of the number of positive charges.¹²

Chitosan is derived by deacetylation of the naturally occurring polysaccharide chitin. Due to its biodegradability, chitosan is now emerging as a polycation for non-viral gene delivery.^{13–16} The charge density of chitosan can be controlled by the fraction of deacetylated units along the chain and offers a way to control the interaction with polyanions. In this study the influence of charge density on the complex formation is investigated in two ways. A set of chitosans with the same valence but differing in their charge densities have been employed to address the question whether the polycation valence is the important parameter to control, or if also the charge density plays a role

Table 1. Chitosans Employed for the Compaction Studies

F_A	\sim DP	term used for identification
0.01	460	C(0.01, 460)
0.49	1030	C(0.49, 1030)
<0.002	100	C(<0.002, 100)
0.49	250	C(0.49, 250)

in the compaction process. Furthermore, the charge densities of the chitosans have been varied by carrying out the complexation at two different pH values, below and above the chitosan pKa (pKa of 6.5^{17,18}). The chitosans employed are related to a series of chitosans previously investigated with respect to their potential as a carrier in gene delivery.¹⁹ In order to further understand the general aspects of polyelectrolyte complexation and in particular the influence of the polycation charge density and valence, this study also includes investigations of the complexation between xanthan and chitosan. Looking at the compaction of DNA from a general perspective can be of help to understand the polyelectrolyte complexation process per se, which is also of importance for the improvement for polycation-based gene delivery systems.

Materials and Methods

Biopolymer Samples. The plasmid DNA pBR322 (4363bp, Böhning Mannheim) was used for all AFM studies. For the additional size measurements and Ethidium Bromide fluorescence measurements, the linear calf thymus DNA (~ 10 kbp, D-1501, Sigma Aldrich) was employed. Xanthan ($M_w 5 \times 10^6$ g/mol) was purified from a fermentation broth (Statoil, Bioferm, Norway).²⁰ Two different sets of chitosans were employed (kindly provided by Dr. Sabina Strand, Dept. of Biotechnology, NTNU). Each set consists of two chitosans with approximately equal valence (charge per polymer chain) but differing in their degree of acetylation (F_A), thus providing chitosans of different charge densities. The two sets of chitosans differed in the degree of polymerization (DP), one set representing chitosans with a high DP, while the other set of chitosans had a low DP. The details of the chitosan samples are summarized in Table 1. The DNAs were dissolved in Tris-EDTA buffer, pH 7, while xanthan and chitosans were dissolved in

* Author to whom correspondence should be addressed. Fax: +47 73 59 77 10. E-mail: bjorn.stokke@phys.ntnu.no.

[†] The Norwegian University of Science and Technology.

[‡] University Hospital of Trondheim.

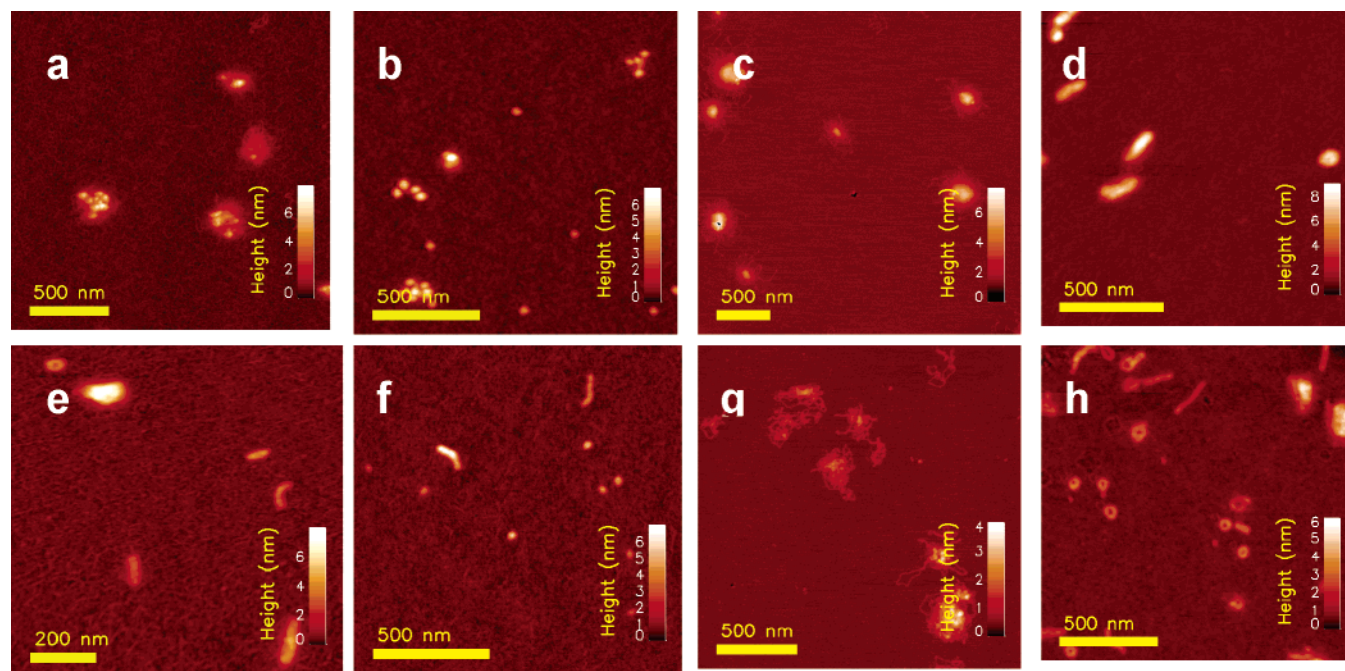


Figure 1. Tapping mode AFM topographs of pDNA–chitosan complexes employing a set of high degree of polymerization chitosans with different charge density but approximately equal total valence. The compaction has been carried out at two different pHs and different charge ratios, with the compaction conditions being (A) C(0.01, 460) 150 mM pH7.4 $k = 0.9$; (B) C(0.01, 460) 150 mM pH7.4 $k = 6$; (C) C(0.01, 460) 150 mM pH5.5 $k = 0.9$; (D) C(0.01, 460) 150 mM pH5.5 $k = 6$; (E) C(0.49, 1030) 150 mM pH7.4 $k = 0.9$; (F) C(0.49, 1030) 150 mM pH7.4 $k = 6$; (G) C(0.49, 1030) 150 mM pH5.5 $k = 0.9$; (H) C(0.49, 1030) 150 mM pH5.5 $k = 6$.

MQ-water, all to a stock solution of 1 mg/mL. The polymers were further diluted in ammonium acetate (NH_4Ac) at an ionic strength of 150 mM (DNA compaction studies), pH 5.5 or pH 7.4, or ionic strength of 5 mM, pH 5.5 (xanthan compaction).

Complex Formation Studied by AFM Imaging. Complexes were formed by adding the chitosan solution to the polyanion solution (equal volumes) yielding a final polyanion concentration of 3–5 $\mu\text{g}/\text{mL}$. Complexation was carried out at a charge ratio (\pm)(k) of 0.9 and 6 for DNA–chitosan and $k = 3$ for xanthan–chitosan. The charge ratio was calculated as the ratio between the number of amine groups on chitosan (adjusted for pH^9) and the number of negatively charged groups on the polyanion. The complexation process was allowed to proceed for 30 min before samples for AFM imaging were prepared. AFM samples were prepared and imaged by tapping mode AFM (Digital Instrument Multimode IIIa) in air as described previously.²⁰ The AFM topographs were subject to quantitative analysis, based on the calculation of a shape factor, the asphericity index, for each structure in the topographs.²⁰ Several topographs were included in the analysis of distribution of morphologies and their dimensions with a number of complexes observed by AFM for each preparation conditions included in the analysis being in the range 50 to 250.

Ethidium Bromide Exclusion Assay. The complexation of DNA with the different chitosans was studied by the ethidium bromide fluorescence assay. Ethidium bromide (EtBr, Sigma Aldrich) is a fluorescent probe whose fluorescence quantum yield is increased upon intercalation into the DNA helix.²¹ Condensation of DNA results in a decreased fluorescence signal, as the EtBr is expelled from the DNA–EtBr complex. EtBr was added to the DNA solution (5 $\mu\text{g}/\text{mL}$) to yield one dye molecule for every second DNA base pair. The fluorescence was measured in 1.5 mL cuvettes using a Spex Spectramate Fluorolog (Spex Industries, Inc., Metuchen, NJ). The excitation wavelength, λ_{ex} , was 511 nm, and the emission spectrum was recorded up to 700 nm. A measure of the fluorescence intensity was obtained from the spectrum by calculating the average intensity within the wavelength interval 595–610 nm. The compaction of DNA by the different chitosans was investigated by recording the fluorescence signal following stepwise addition of chitosan at time intervals of ~ 15 min. In reporting the titration curves, the fluorescence intensity was normalized relative to

the fluorescence intensity of DNA–EtBr before addition of chitosan without subtracting the background fluorescence.

Size Measurements. The sizes of the polyelectrolyte complexes were measured by employing dynamic light scattering (Zetasizer Nano, Malvern Instrument). Two independent samples ($C_{\text{DNA}} = 5\text{--}10 \mu\text{g}/\text{mL}$) were measured with a minimum of three parallel runs of each sample. The data were analyzed both in terms of z -average size and number-average size.

Results

Characterization of DNA–Chitosan Complexes: High DP Chitosans. Two chitosans with high degree of polymerization (high DP) and equal valence (charge per polymer chain); C(0.01, 460) and C(0.49, 1030) were chosen to investigate whether the charge density (determined by the F_A) or only the cation valence is important in determining the complexation behavior upon mixing with a polyanion such as DNA. Measurements of the z -average and number average diameter of the polyplexes utilizing dynamic light scattering revealed in general no large differences when employing the chitosans C(0.01,460) and C(0.49, 1030) to compact DNA at the two different pHs (data not shown). One exception was the DNA–C(0.49, 1030) complexes formed at pH 5.5, $k = 0.9$, where the diameter of the polyplexes was found to greatly exceed that of the other systems.

However, as reported previously,⁹ DNA compaction with chitosans results in a blend of structures: toroids, rods, and globules, with the relative amounts of the different structures depending on the actual chitosan, charge ratio, and solution properties like pH and ionic strength. The complexation behavior of the chitosans was therefore further investigated by visualization by AFM. As illustrated in the AFM topographs (Figure 1), the structures resulting from the complexation depended on both the pH and the charge ratio (\pm). For the high DP chitosan pair, at high pH, the chitosan C(0.49, 1030) was able to compact the

DNA into rods, a few toroids and additionally globular structures (pH 7.4) at both charge ratios ($k = 0.9, 6$, panels E and F, respectively, of Figure 1). In contrast to this, the chitosan C(0.01, 460) resulted in mainly globular structures at both charge ratios (pH 7.4), with the globules tending to aggregate. At $k = 0.9$ (Figure 1A) some of the globules/aggregates were found to possess a “hairy” shell of polymer surrounding the complexes. For $k = 6$ (Figure 1B) a few rodlike structures could also be observed; however, at this compaction condition the structures were dominantly small globules.

When the pH was reduced to 5.5, the apparent efficiency of the high DP chitosans to induce complexation also changed. At this pH neither of the high DP chitosans were able to fully compact the DNA when employing a charge ratio of $k = 0.9$ (Figure 1C,G), a charge ratio that induced complexation to well-defined structures at pH 7.4. In addition to having DNA chains protruding from the structures, uncomplexed DNA could also be observed. Increasing the charge ratio to $k = 6$, the chitosan C(0.01, 460) compacted DNA into rods and globules, as well as some toroids, with a very small inner radius (hole) (Figure 1D). Similar to compaction with this chitosan at pH 7.4, $k = 0.9$ (Figure 1A), some of the structures observed at this condition were surrounded by a brushy polymer layer. At this high charge ratio also C(0.49, 1030) compacted DNA into well-defined structures, mainly toroids and rods, and hardly any globular structures at all (Figure 1H). In this case the inner radii of the toroids were much larger than observed when employing C(0.01, 460) (Figure 1D).

Characterization of DNA–Chitosan Complexes: Low DP Chitosans. The complexation behavior was also studied for another pair of chitosans with approximately equal valence but low DP, namely the chitosans C(<0.002, 100) and C(0.49, 250). For this pair of chitosans, the complexation with DNA was carried out only at pH 7.4 and at a charge ratio of $k = 6$ (Figure 2). Neither of the chitosans resulted in toroidal complexes when mixed with DNA at this condition. The chitosan C(<0.002, 100) compacted DNA into globules and rods (Figure 2A), while complexation of DNA with C(0.49, 250) resulted predominantly in globular structures, with the appearance of a few rodlike complexes (Figure 2B).

Quantitative Analysis of DNA–Chitosan Complexes: High DP Chitosans. The DNA–chitosan structures were classified into four different groups depending on their asphericity index. Toroids were defined to have an $A = (0.2–0.35)$ with the additional criteria of a visible height minimum in the center and rods were defined to have $A > 0.5$. Due to tip-convolution, globular structures are not found at the ideal value of $A = 0$, but coexist in the same region as the toroids, and this group was therefore defined as structures with $A < 0.35$, excluding toroids. The remaining structures, not being classified as either of the above, were categorized as “others.” To this group belonged mainly two different types of structures: aggregates of globules, as well as small aggregates with a not well-defined shape. The toroids and rods were further analyzed to give height and contour length distributions of the structures.

Since DNA was not fully compacted at a charge ratio of 0.9 at pH 5.5, this condition was not subject to any analysis. Analysis of the polyplexes formed at a charge ratio $k = 6$, pH 5.5, showed little difference between C(0.01, 460) and C(0.49, 1030) when it came to the relative amount of different structures (Figure 3A).

Increasing the pH to 7.4, both chitosans were found to compact DNA to well-defined structures at both of the employed charge ratios (0.9 and 6). However, in both cases toroids were

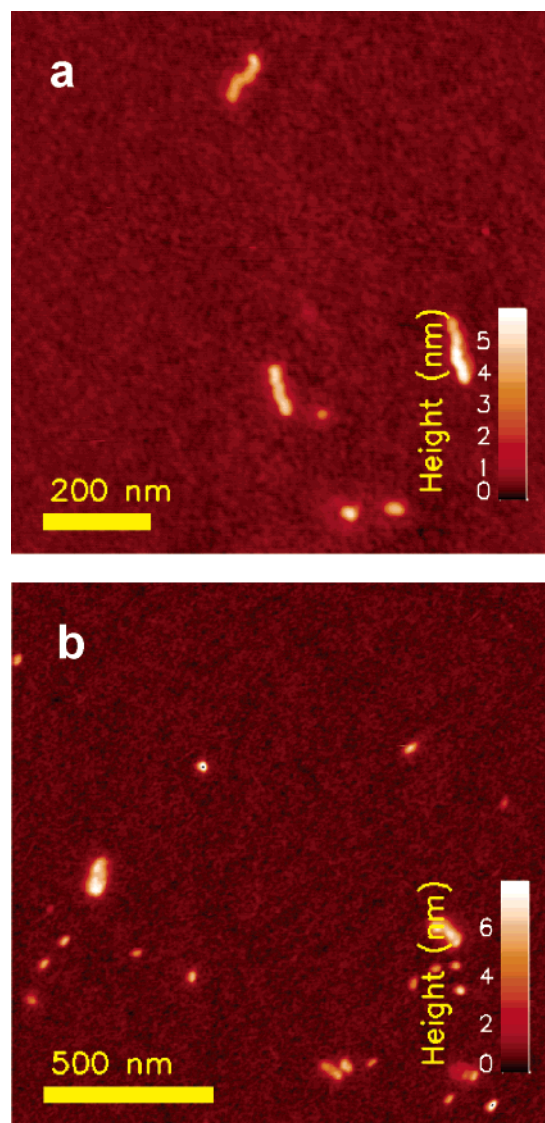


Figure 2. AFM images of pDNA–chitosan complexes employing a set of low DP chitosans with different charge density but \sim equal total valence. The compaction conditions being (A) C(<0.002, 100) 150 mM pH 7.4 $k = 6$; (B) C(0.49, 250) 150 mM pH 7.4 $k = 6$.

formed only when C(0.49, 1030) was employed for compaction. Although compaction of DNA with C(0.01, 460) resulted in some linear complexes, analysis revealed that this chitosan, at both charge ratios investigated, mainly resulted in globular structures upon complexation with DNA (Figure 3). For DNA–C(0.49, 1030) complexes, globular structures were also found to constitute a large fraction of the structures at a charge ratio of $k = 6$.

For the conditions where comparison was possible, it was found that the width of the height distribution was broader for the linear structures formed by compaction with chitosan with high F_A (0.49) compared to the low F_A chitosan (Table 2). The width of the height distribution is here defined as the width between the fifth and 95th percentile. For the one condition where both chitosans produced an analysable fraction of toroids (pH 5.5, $k = 6$) the C(0.49, 1030) resulted in a narrower height distribution than C(0.01, 460) (4.7 nm compared to 8.5 nm respectively).

Quantitative Analysis of DNA–Chitosan Complexes: Low DP Chitosans. For the second pair of chitosans (C(<0.002, 100) and C(0.49, 250)), neither resulted in any toroidal complexes

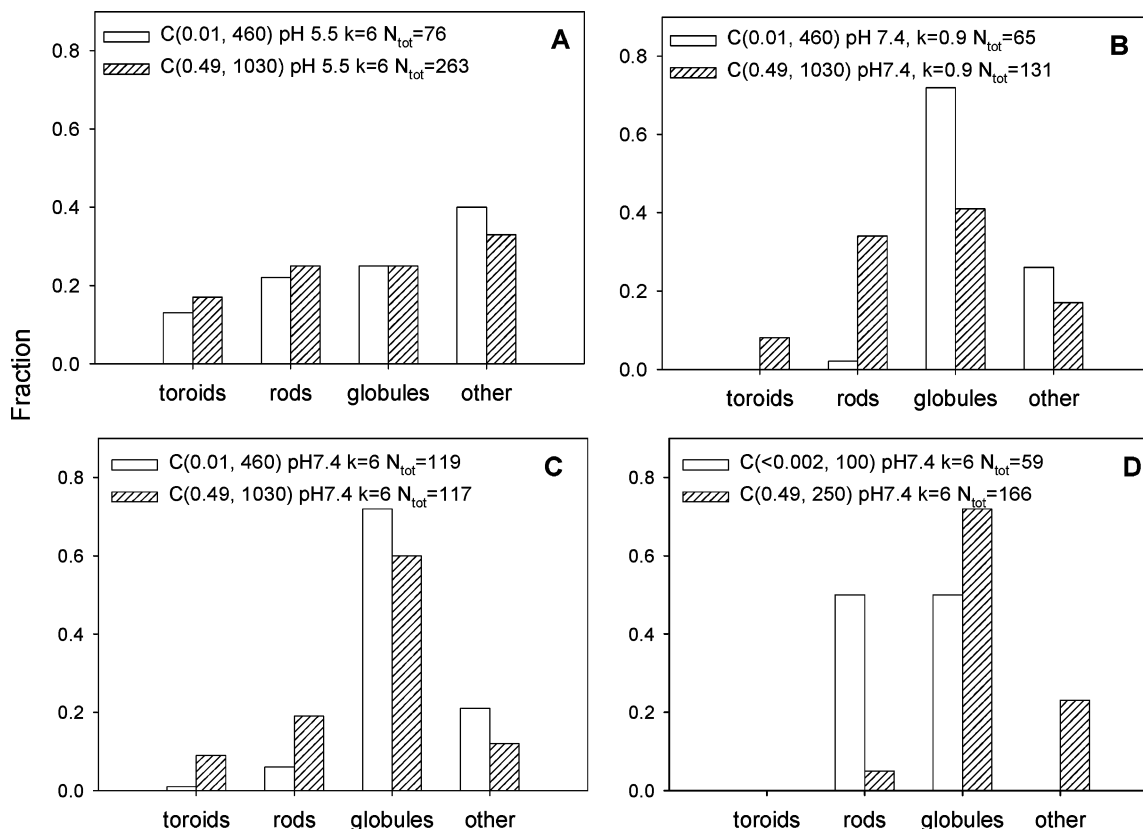


Figure 3. Comparison of the amount of different structures formed when chitosans of different charge densities but approximately equal valence has been employed to compact pDNA.

Table 2. Width of Height Distributions for Compacted DNA–Chitosan Structures, Calculated as the Width between the fifth and 95th Percentile

chitosan	pH	charge ratio k	toroids ^a (width, nm)	rods (width, nm)
C(0.49, 1030)	5.5	6	4.7	5.9
	7.4	0.9	14.0	7.0
	7.4	6	6.0	8.5
C(0.01, 460)	5.5	6	8.5	4.7
	7.4	6	—	4.9
C(0.49, 250)	7.4	6	—	7.6
C(<0.002, 100)	7.4	6	—	6.0

^a There was not an analysable fraction of toroids for all conditions.

when mixed with DNA at the condition investigated (150 mM, pH 7.4, $k = 6$) (Figure 3D). For DNA–C(<0.002, 100) the resulting complexes were found to fall into the categories rods and globules, with approximately equal amount of the two types of structures. Hardly any rods were observed when employing C(0.49, 250) for the DNA compaction, compaction with this chitosan resulted in predominantly globular structures.

The width of the height distribution was also for this pair of chitosans found to be broader for the linear structures formed by compaction with high F_A (0.49) compared to the low F_A (Table 2).

DNA–Chitosan Compaction Monitored by EtBr Fluorescence. Displacement of EtBr from its intercalated position within the DNA associated with the DNA–chitosan interaction was used to determine relative interaction strength of the chitosans with DNA. Titration curves like this have been employed to deduce the association constant,^{22,23} and the charge ratio required to achieve a minimum fluorescence signal has

been taken as a relative measure of the interaction strength, with higher charge ratios indicating lower interaction strengths.²⁴

Comparison of the different chitosans revealed that they had different efficiencies in expelling the EtBr from the DNA helix, and that this also depends on the DP of the chitosan (Figure 4). The slope of the relative fluorescence intensity with increasing charge ratio as chitosan is titrated to DNA and the A/P ratio at which the fluorescence intensity reaches a plateau value (referred to as the transition charge ratio) are used to compare the compaction efficiency of the different chitosans (Table 3). Both values give an indication of the relative association constants between DNA and the chitosans, with steep slope and low transition charge ratio indicating a strong association.

For the low DP chitosans, both the slope and the transition charge ratio was approximately the same at the low pH (Table 3), while the chitosan with the lowest F_A , C(<0.002, 100), was most efficient in expelling EtBr at the high pH (Figure 4A), having a steeper slope (0.43) compared to C(0.49, 250) (slope of 0.26). Both the slope and the transition charge ratio for which a minimum fluorescence intensity was reached indicate that in the low DP chitosan pair, the binding is strongest between DNA and the chitosan with the highest charge density, C(<0.002, 100).

For compaction of DNA with the high DP chitosans at pH 5.5, the lowest charge ratio for which a plateau of minimum fluorescence intensity was reached was observed when employing the chitosan C(0.49, 1030) (Table 3). Both chitosans have a steeper slope at the low pH than the high, reaching the plateau value at a smaller charge ratio at pH 5.5 than at pH 7.4 (Table 3). Hence, common for both high DP chitosans are that they, as measured by the fluorescence assay, are more efficient at compacting DNA at the low pH (5.5) as compared to the high pH (7.4). At the high pH, the transition charge ratio at which

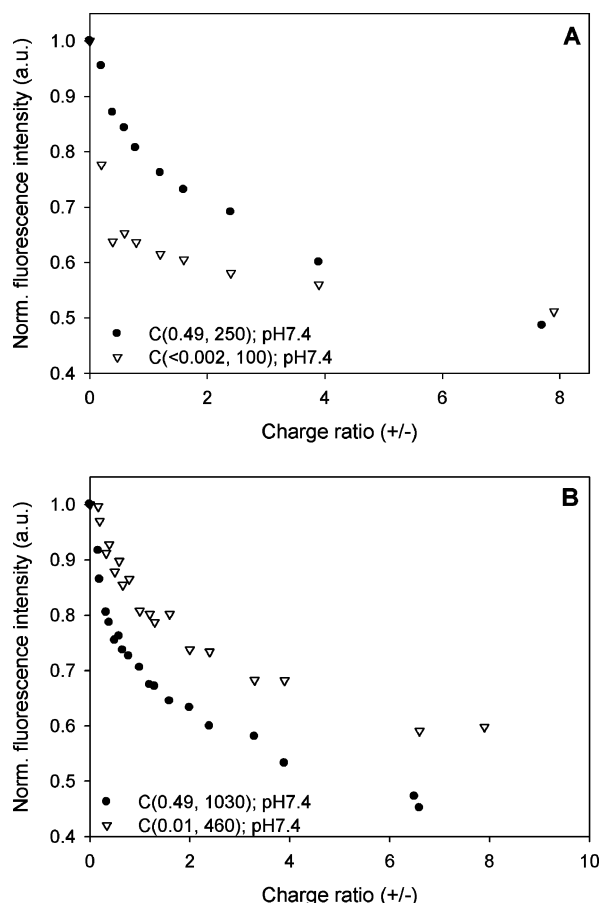


Figure 4. Titration curves when the different chitosans were titrated to a solution of EtBr and DNA. The DNA employed was the calf thymus DNA, and the experiments were carried out in 150 mM ammonium acetate pH 7.4. (A) Titration of the set of low DP chitosans and (B) titration of the set of high DP chitosans.

the plateau value is reached is above 7 for both chitosans, indicating that even at this charge ratio the DNA is not fully compacted. Similar to pH 5.5, at pH 7.4 the chitosan C(0.49, 1030) gives rise to a steeper slope in the fall of fluorescence intensity than C(0.01, 460), Figure 4B, indicating that the

Table 3. The Charge Ratio at Which the Relative Fluorescence Intensity Reaches Its Plateau Value (Transition Charge Ratio) as Well as the Slope of the EtBr Titration Curve below $k = 1.0$ for the Titration of Chitosan to DNA

chitosan	pH	transition charge ratio	slope, $k/(0, 1.0)$
C(0.49, 1030)	5.5	~ 1.5 –2	0.48
C(0.49, 1030)	7.4	> 7	0.31
C(0.01, 460)	5.5	~ 4	0.22
C(0.01, 460)	7.4	> 8	0.20
C(0.49, 250)	5.5	~ 2	0.40
C(0.49, 250)	7.4	> 8	0.26
C(<0.002, 100)	5.5	~ 1.5	0.44
C(<0.002, 100)	7.4	~ 0.5	0.43

association between DNA and high DP chitosans is stronger for the chitosan of low charge density, C(0.49, 1030).

Xanthan–Chitosan Complexes. Xanthan compacted with C(0.49, 1030) resulted in similar structures as those observed previously for xanthan compaction,²⁰ with a fraction of toroids of 0.25 and additionally a number of other structures, referred to as metastable structures, characterized by loops, such as racquets (Figure 5). When C(0.01, 460) was employed to compact xanthan, the fraction of toroids increased to 0.52, concomitant with a decrease in the fraction of metastable structures. Analysis of the toroidal fraction furthermore showed that the toroids formed between C(0.01, 460) and xanthan were thicker (3.8 ± 1.6 nm, $N = 117$) than those formed between xanthan and C(0.49, 1030) (2.0 ± 0.6 nm, $N = 193$), Figure 6A. The toroids formed by xanthan compacted by C(0.49, 1030) were found to have an average contour length of 250 ± 72 nm. For xanthan–C(0.01, 460) the contour length took a broader distribution, extending from ~ 200 nm to 450–500 nm (Figure 6B). This could also be observed in the AFM topographs where it appeared to be two distributions of toroids in terms of their apparent diameter.

Discussion

Polyelectrolyte complexation is of importance in a number of areas, and understanding the parameters influencing the complexation process is therefore of interest. This study

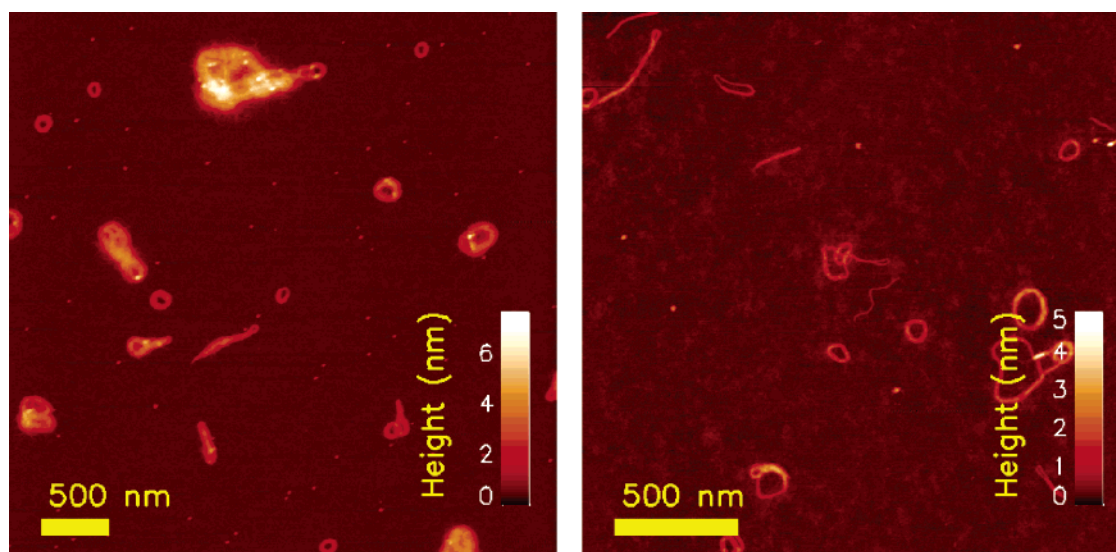


Figure 5. AFM images of chitosan compacted xanthan, employing two different chitosans with different charge densities but approximately equal valence, with the compaction being carried out at 5 mM pH 5.5 and a charge ratio (chitosan/xanthan) of 3. (A) Compaction with the chitosan C(0.01, 460) and (B) compaction with the chitosan C(0.49, 1030).

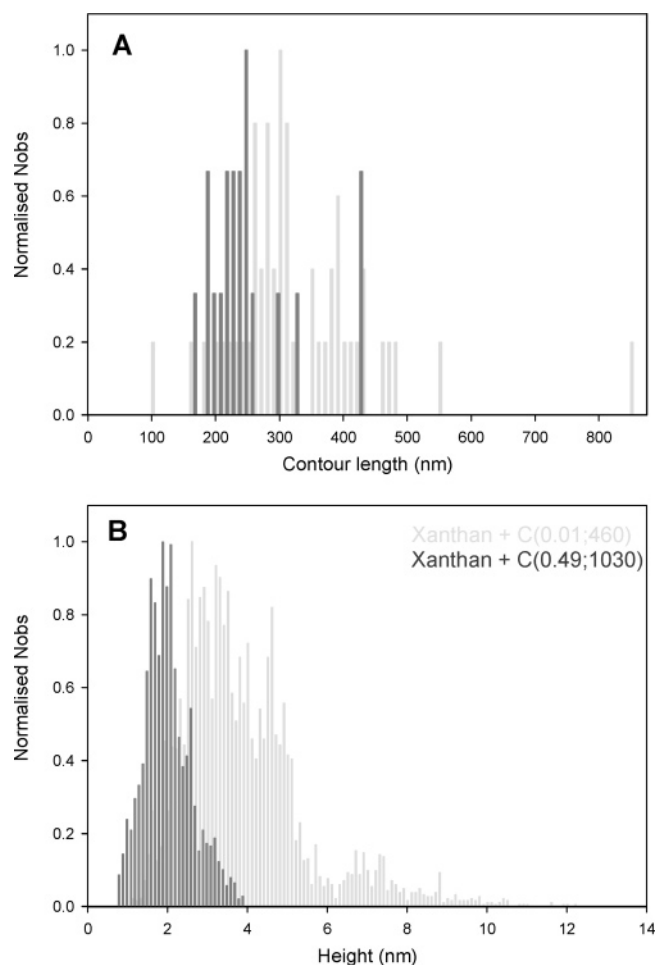


Figure 6. (A) Contour length and (B) height distributions of xanthan–chitosan toroids, comparing the two different chitosans C(0.001, 460) and C(0.49, 1030). The compaction was carried out at 5 mM pH5.5 and a charge ratio (chitosan/xanthan) of 3.

addresses the relative importance of polycation charge density and total valence in the complexation of oppositely charged polyanions. This has been carried out by studying the complexation of different polyanions (xanthan and DNA) with chitosans of different charge densities and approximately equal valence. From the present EtBr and AFM data, it is found that the valence is not the only important parameter determining the formation of polyelectrolyte complexes. The charge density of the polycation is also an important parameter, influencing both the apparent interaction strength as well as the type of morphologies of the structures formed. However, the charge density cannot be viewed as an independent parameter, as its influence on the compaction process appears to be connected with the chain length (DP) of the polycation. More specifically at high pH (7.4), it is found that for the low DP chitosans the interaction strength is strongest for the high charge density chitosan ($C(<0.002, 100)$). Increasing the DP of the chitosans results in the low charge density chitosan (C(0.49, 1030)) binding stronger to DNA than the chitosan of high charge density. The data therefore clearly show that there is interplay between the charge density, total valence and DP. Furthermore, the AFM data, when compared with the EtBr data, is in the following suggested to provide information about how a high interaction strength (low pH) can contribute to a kinetic trapping of structures.

For the pair of low DP chitosans in this study, we find that the chitosan with highest charge density, C($<0.002, 100$), binds stronger to DNA than C(0.49, 250). This is in accordance with literature, where the binding constant between a ligand and an

oppositely charged polymer has been shown to depend upon the valence of the ligand.^{10,11} It has also been shown that the number of positive charges is important for the efficiency of polycations as gene delivery vehicles.^{25,26} It has been suggested that a lower density of amino groups in chitosans of decreased M_w or lower degree of deacetylation (i.e., higher F_A) could lead to weaker association between DNA and chitosan.^{9,24,27} Studies employing synthetic copolymers with varying charge densities have reported that the interaction strength with DNA increase with increased charge density of the copolymer,²⁸ while chemical modification to decrease the charge density of poly-L-lysine reduced the capacity of poly-L-lysine to induce DNA condensation.²⁹ One of the driving forces of polyelectrolyte complexation is the release of counterions from the polyanion–polycation pair, increasing the entropy of the system.^{2,3} In this perspective, increasing the charge density of the polycation, more counterions can be released per polycation chain binding to the polyanion increasing the entropy of the system leading to a stronger binding. This is in accordance with NMR studies of the interaction between DADMAC-AA copolymers and PSS, where DADMAC-AA copolymers with higher charge density were found to restrict the positions of the counterions to a large degree, thus offering larger entropy gain when releasing them into solution.³⁰ Monte Carlo simulation studies have also shown that a reduction in linear charge density of a polyelectrolyte reduced the capacity to condense macroions.³¹

Increasing the chain length of the chitosan, the influence of the charge density is changed. Contrasting the two high DP chitosans investigated here, C(0.01, 460) and C(0.49, 1030), the EtBr fluorescence assay show that C(0.01, 460) is less efficient in expelling EtBr from the DNA helix than C(0.49, 1030). The titration curves obtained for the two chitosans therefore indicate that, at both pHs investigated, the interaction between DNA and C(0.01, 460) is weaker than that between DNA and C(0.49, 1030). For high molecular weight chitosan, the present data suggest that increasing the charge density (decreased F_A) leads to a decreased affinity between chitosan and DNA. This is evident in the EtBr-assay where a reduction in F_A results in less EtBr being expelled (i.e., higher residual fluorescence level). Hence, for high DP chitosans, the increased release of counterions following from increased charge density, appear to be of less importance than for low DP chitosans. It is likely that the restriction of the polycation chain upon complexation becomes more important, giving rise to different complexation behavior than for the low DP chitosan pair.

It has previously been shown that the toroid represent a low energy state of the xanthan–chitosan complexes.³² Assuming this is a general behavior for xanthan–chitosan systems, the increased fraction of toroids observed with C(0.01, 460) as compared to C(0.49, 1030) indicates that the former induces a more stable state. The increased toroidal height is also in accordance with previous studies of xanthan–chitosan complexes and the kinetically stable state. This might be an indication of the interaction strength between xanthan and C(0.01, 460) being smaller, and thereby this xanthan–chitosan system is not trapped in metastable states to the extent the xanthan–C(0.49, 1030) system is. This is in support of the hypothesis presented above for the DNA–chitosan studies.

The second approach to changing the charge density of chitosan is to study the complexation at different pHs. Decreasing the pH from 7.4 to 5.5 increased the chitosan induced displacement of EtBr from DNA for both C(0.49, 1030) and C(0.01, 460). On the basis of the EtBr assay the binding between DNA and chitosan is therefore believed to be stronger at lower

pH, as could be expected from the increased degree of ionization of chitosan at low pH. This is in accordance with another study, where the ionization of a weakly charged synthetic polymer (DMAEMA) has been changed by changing the solution pH during complexation with DNA. The study concluded that the increased charge density resulting from a lowering of pH leads to greater binding affinities between the DMAEMA polymer and DNA.³³ AFM imaging showed that at a charge ratio of $k = 0.9$ (\pm), DNA chains can be seen protruding from the complexes at the low pH (5.5) for both investigated chitosans. Since the EtBr assay indicates that the affinity between DNA and chitosan is larger at this pH than at pH 7.4 where complexes with fully condensed DNA are observed, it is likely that the complexes at pH 5.5 represent complexes where the interaction traps the DNA before it is able to fully relax into a compacted form.

Furthermore, a charge ratio k (\pm) of 0.9 may not be sufficiently large to result in fully compacted DNA. It has previously been reported that a 90% charge neutralization is necessary for DNA condensation.³⁴ The AFM studies also show that at a higher pH (7.4) DNA is fully compacted at $k = 0.9$, in accordance with previous studies. However, it has also been suggested that polycations such as chitosan will undergo protonation in the presence of polyanions. At pH 7.4, above the pKa of chitosan,^{17,18} only a few of the amine groups are protonated, thus a large excess of chitosan is needed to reach a charge ratio of 0.9. If chitosan is being protonated in the presence of DNA, the equilibrium will be shifted so that the actual charge ratio is higher than 0.9. This in turn might result in DNA being fully compacted at the low charge ratio only at the high pH and not at the low, where all potential groups are protonated, leaving no potential to increase the actual charge ratio in the polyplex solution.

Conclusion

Chitosan is one potential polycation for gene delivery purposes. To further understand the complexation process, the influence of charge density of chitosans on the polyanion–polycation process has been studied employing different techniques. Even though size measurements do not reveal major differences when chitosans with different charge densities but approximately equal total charge are employed to compact DNA, AFM studies show that the different chitosans result in different ratios of structures of the polyelectrolyte complexes. This is also substantiated by compaction of a second polyanion, xanthan. Hence, not only the total valence, but also the charge density of the polycation is of importance in the complexation process. The influence of charge density is found to be linked to the degree of polymerization of the chitosans, with short chitosans binding stronger at a high charge density, while long chitosans bind stronger when the chitosan charge density is low. Furthermore, this study shows that studies of individual particles, as by AFM imaging, might reveal important differences not detected in studies of solution average properties.

Acknowledgment. This work is supported by The Norwegian Research Council (grant number 166794/V30). We thank Dr. Sabina Strand, Dept. of Biotechnology, NTNU, Norway for providing the chitosan samples. The assistance of Kristin

Sæterbø in carrying out some of the experiments is gratefully acknowledged.

References and Notes

- Thünemann, A. F.; Müller, M.; Dautzenberg, H.; Joanny, J.-F.; Löwen, H. *Adv. Polym. Sci.* **2004**, *166*, 113–171.
- Manning, G. S. *Q. Rev. Biophys.* **1977**, *11*, 179–246.
- Matulis, D.; Rouzina, I.; Bloomfield, V. A. *J. Mol. Biol.* **2000**, *296*, 1053–1063.
- Merdan, T.; Kopecek, J.; Kissel, T. *Adv. Drug Delivery Rev.* **2002**, *54*, 715–758.
- Philipp, B.; Dautzenberg, H.; Linow, K.-J.; Kötter, J.; Dawydoff, W. *Prog. Polym. Sci.* **1988**, *14*, 91–172.
- Gosule, L. C.; Schellman, J. A. *Nature* **1976**, *259*, 333–335.
- Arcsott, P. G.; Li, A.-Z.; Bloomfield, V. A. *Biopolymers* **1990**, *30*, 619–630.
- Kwoh, D. Y.; Coffin, C. C.; Lollo, C. P.; Jovenal, J.; Banaszczuk, M. G.; Mullen, P.; Phillips, A.; Amini, A.; Fabrycki, J.; Bartholomew, R. M.; Brostoff, S. W.; Carlo, D. J. *Biochim. Biophys. Acta* **1999**, *1444*, 171–190.
- Danielsen, S.; Vårum, K. M.; Stokke, B. T. *Biomacromolecules* **2004**, *5*, 928–936.
- Plum, G. E.; Arcsott, P. G.; Bloomfield, V. A. *Biopolymers* **1990**, *30*, 631–643.
- Mascotti, D. P.; Lohman, T. M. *Proc. Natl. Acad. Sci. U. S. A.* **1990**, *87*, 3142–3146.
- Köping-Höggård, M.; Mel'nikova, Y. S.; Vårum, K. M.; Lindman, B.; Artursson, P. *J. Gene Med.* **2003**, *5*, 130–141.
- MacLaughlin, F. C.; Mumper, R. J.; Wang, J.; Tagliaferri, J. M.; Gill, I.; Hinchcliffe, M.; Rolland, A. P. *J. Controlled Release* **1998**, *56*, 259–272.
- Erbacher, P.; Zou, S.; Bettinger, T.; Steffan, A.-M.; Remy, J. S. *Pharm. Res.* **1998**, *15*, 1332–1339.
- Richardson, S. C. W.; Kolbe, H. V. J.; Duncan, R. *Int. J. Pharm.* **1999**, *178*, 231–243.
- Lee, M.; Nah, J. W.; Kwon, Y.; Koh, J. J.; Ko, K. S.; Kim, S. W. *Pharm. Res.* **2001**, *18*, 427–431.
- Anthonsen, M. W.; Smidsrød, O. *Carbohydr. Polym.* **1995**, *26*, 303–305.
- Strand, S. P.; Tømmersaas, K.; Vårum, K. M.; Østgaard, K. *Biomacromolecules* **2001**, *2*, 1310–1314.
- Köping-Höggård, M.; Tubulekas, I.; Guan, H.; Edwards, K.; Nilsson, M.; Vårum, K. M.; Artursson, P. *Gene Ther.* **2001**, *8*, 1108–1121.
- Maurstad, G.; Danielsen, S.; Stokke, B. T. *J. Phys. Chem. B* **2003**, *107*, 8172–8180.
- LePecq, J.-B.; Paoletti, C. *J. Mol. Biol.* **1967**, *27*, 87–106.
- Zelikin, A. N.; Trukhanova, E. S.; Putnam, D.; Izumrudov, V. A.; Litmanovich, A. A. *J. Am. Chem. Soc.* **2003**, *125*, 13693–13699.
- Cain, B. F.; Baguley, B. C.; Denny, W. A. *J. Med. Chem.* **1978**, *21*, 658–668.
- Danielsen, S.; Strand, S.; Davies, C. L.; Stokke, B. T. *Biochim. Biophys. Acta* **2005**, *1721*, 44–54.
- Erbacher, P.; Roche, A. C.; Monsigny, M.; Midoux, P. *Biochim. Biophys. Acta* **1997**, *1324*, 27–36.
- Putnam, D.; Gentry, C. A.; Pack, D. W.; Langer, R. *Proc. Natl. Acad. Sci. U. S. A.* **2001**, *98*, 1200–1205.
- Huang, M.; Fong, C.-W.; Khor, E.; Lim, L.-Y. *J. Controlled Release* **2005**, *106*, 391–406.
- Fischer, D.; Dautzenberg, H.; Kunath, K.; Kissel, T. *Int. J. Pharm.* **2004**, *280*, 253–269.
- Miyata, K.; Kakizawa, Y.; Nishiyama, N.; Harada, A.; Yamasaki, Y.; Koyama, H.; Kataoka, K. *J. Am. Chem. Soc.* **2004**, *126*, 2355–2361.
- Kriz, J.; Dautzenberg, H. *J. Phys. Chem. A* **2001**, *105*, 3846–3854.
- Jonsson, M.; Linse, P. *J. Chem. Phys.* **2001**, *115*, 3406–3418.
- Maurstad, G.; Stokke, B. T. *Biopolymers* **2004**, *74*, 199–213.
- Rungsardthong, U.; Ehtezazi, T.; Bailey, L.; Armes, S. P.; Garnett, M. C.; Stolnik, S. *Biomacromolecules* **2003**, *4*, 683–690.
- Wilson, R. W.; Bloomfield, V. A. *Biochemistry* **1979**, *18*, 2196.

BM0610119